

# The Effects of Notch Width on the SENB Toughness for Oxide Ceramics

J. Wang

IRC in Materials for High Performance Applications, The University of Birmingham, Birmingham, UK, B15 2TT

W. M. Rainforth

School of Materials, The University of Sheffield, Sheffield, UK, S1 3JD

I. Wadsworth & R. Stevens\*

School of Materials, The University of Leeds, Leeds, UK, LS2 9JT

(Received 23 August 1991; revised version received and accepted 29 October 1991)

## Abstract

*The fracture toughness of a range of oxide ceramics, namely aluminas with various grain sizes,  $Y_2O_3$ -stabilized tetragonal zirconia polycrystals (Y-TZP), MgO-partially stabilized zirconias (Mg-PSZ) and zirconia-toughened ceramics (ZTC), has been measured by the single edge notch beam (SENB) technique using machined notches of varying widths from 150 to 1800  $\mu\text{m}$ . It was found that the response of each material was critically dependent on its microstructure. Experimental results show that where 'dynamic' toughening mechanisms occur, such as transformation toughening, SENB toughness depends strongly on the notch width. For example, the SENB toughness of  $Y_2O_3$ -stabilized tetragonal zirconia polycrystals and MgO-partially stabilized zirconia ceramics, which are typical of transformation toughened ceramics, increases significantly with increasing notch width when the notch width is less than 1 mm. A further increase in the notch width results in only a slight increase in the SENB toughness. Zirconia-toughened alumina (ZTA) ceramics show similar behaviour, although the increase in SENB toughness is smaller than that for Y-TZP ceramics. The notch width dependence of SENB toughness for the transformation toughened ceramics is related to the transformation zone at the notch tip, induced by diamond blade machining. In contrast, the SENB toughness of alumina ceramics shows very little response to the variation in notch*

*width. A discussion on the relationships between SENB toughness values measured and the operative toughening mechanisms is presented.*

*Die Bruchzähigkeit einer Reihe verschiedener oxidischer Keramiken, nämlich von Aluminiumoxid mit verschiedenen Korngrößen, von polykristallinem  $Y_2O_3$ -stabilisiertem Zirkoniumoxid (Y-TZP), von MgO-partiell-stabilisiertem Zirkoniumoxid (Mg-PSZ) und von Zirkoniumoxid-verstärkten Keramiken (ZTC) wurde an einseitig gekerbten Biegebruchstäbchen (SENB) gemessen, wobei vorher jeweils verschiedene Kerbweiten von 150 bis 1800  $\mu\text{m}$  eingearbeitet wurden. Es konnte gezeigt werden, daß das Materialverhalten sehr empfindlich vom Gefüge abhängt. Die experimentellen Ergebnisse zeigen, daß für den Fall der 'dynamischen' Zähigkeitssteigernden Mechanismen, wie zum Beispiel Zähigkeitserhöhung durch Umwandlungen, die Kerbbiegebruchzähigkeit stark von der Kerbweite abhängt. So nimmt die Kerbbiegebruchzähigkeit von polykristallinem  $Y_2O_3$ -stabilisiertem Zirkoniumoxid und von mittels MgO-partiell-stabilisiertem Zirkoniumoxid, zwei typischen Vertretern für die Zähigkeitssteigerung durch Umwandlung, drastisch mit zunehmender Kerbweite zu, wenn die Kerbweite geringer als 1 mm ist. Eine weitere Vergrößerung der Kerbweite führt nur zu einer geringen Kerbbiegebruchzähigkeitssteigerung. Zirkoniumoxid-verstärktes Aluminiumoxid (ZTA) zeigt ein ähnliches Verhalten, obgleich die Zähigkeitssteigerung geringer ausfällt als für die Y-TZP-Keramiken.*

\* To whom correspondence should be addressed.

*La résistance à la fracture d'une série de céramiques à base d'oxydes, comme de l'alumine ayant une taille de grain variable, de la zircone polycristalline tétragonale stabilisée par  $Y_2O_3$  (Y-TZP), de la zircone stabilisée partiellement par MgO (Mg-PSZ), et des céramiques renforcées par de la zircone (ZTC), a été mesurée par flexion trois points entaillée (SENB) avec des entailles faite mécaniquement et de largeur varient entre 150 et 1800  $\mu m$ . On a constaté que la réponse de chaque matériau dépend essentiellement de sa microstructure. Les résultats expérimentaux montrent que lorsque le mécanisme de renforcement 'dynamique' se produit, comme le renforcement par transformation de phases, la résistance SENB dépend particulièrement de la largeur de l'encoche. Par exemple la résistance SENB de la zircone polycristalline tétragonale stabilisée par  $Y_2O_3$  et de la zircone stabilisée partiellement par MgO, qui sont typiquement des céramiques qui se renforcent par transformation de phases, augmente de manière significative avec l'augmentation de la largeur de l'encoche quand celle ci reste inférieure à 1 mm. Une augmentation plus importante de la largeur de l'encoche n'amène qu'une faible augmentation de la résistance SENB. Des céramiques à base d'alumine renforcées par de la zircone (ZTA) montrent un comportement similaire, bien que l'augmentation de la résistance SENB est plus petite pour les céramiques Y-TZP. La dépendance de la résistance SENB par rapport à la largeur de l'encoche pour les céramiques renforcées par transformation de phase est reliée à la zone transformation à la pointe de l'encoche, produite par usinage avec une lame de diamant. A l'opposé la résistance SENB des céramiques à base d'alumine est peu influencée par la variation de la largeur de l'encoche. La relation entre les valeurs mesurées de la résistance SENB et les mécanismes intervenant lors du renforcement est discutée.*

## 1 Introduction

Following the discovery of transformation toughening associated with zirconia ceramics,<sup>1-3</sup> there has been considerable progress in developing, understanding and utilizing oxide ceramics. These toughened ceramics are considered to be a new generation of engineering materials with improved mechanical properties. It has been widely appreciated that these oxide ceramics will play an important role in engineering applications in the coming decades.

Engineering design with such ceramic materials requires a full characterization of the mechanical properties. However, such a characterization is

made difficult in the absence of standardized test procedures.<sup>4,5</sup> Moreover, there is increasing evidence that the values which are obtained for the mechanical properties are highly sensitive to the test procedures adopted by each investigator.

Fracture toughness measurement of oxide ceramics is often regarded as ambiguous, and questions remain as to which technique gives the most realistic and reliable result for a particular material. Specifically, one technique is more applicable to certain materials than to others.<sup>6,7</sup> Two techniques are commonly used for the fracture toughness measurement of oxide ceramics, namely Vickers indentation (or microindentation) and single edge notch beam (SENB). For each of these two techniques, there are several experimental parameters which may influence the measured value of the fracture toughness. In the former, the indentation toughness often varies with the indentation load, which is usually selected on the basis of experience.<sup>8-10</sup> The applicability of the indentation technique has been recently questioned, particularly with regard to ceramic materials with very high fracture toughness, such as Y- and Ce-TZP ceramics. In such materials, the crack length at each indent corner is short compared with the dimensions of the indent, even when a relatively high load ( $> 1000$  N) is applied. It is widely accepted that the indentation technique often overestimates the fracture toughness of such highly transformation toughened ceramics, as a consequence of the extensive transformation taking place around the indent.<sup>10,11</sup> The variables which affect the SENB toughness include notch width, sharpness of the notch tip (curvature of the notch tip), length of the notch and the loading rate of specimens during testing.<sup>12,13</sup> Certain materials exhibit a strong SENB toughness dependence on the length of the sharp notch (such as pre-crack). For example, large grain sized alumina ceramics (40  $\mu m$ ) show a considerable rise in the SENB toughness with increasing crack length, possibly as a consequence of a stress-induced microcrack zone developing around the crack tip and the occurrence of crack bridging. Increasing fracture toughness with crack extension known as *R*-curve behaviour has been extensively investigated and detailed in several published papers.<sup>14,15</sup>

Several mechanisms have been suggested to account for the improvements in the mechanical properties of the oxide ceramics already mentioned over those of conventional ceramic materials. These include stress-induced transformation, residual stress generation, stress-induced microcracking,

and crack deflection and bridging.<sup>14,16,17</sup> Such toughening mechanisms can be classified into two main categories,<sup>1,17</sup> namely crack shielding and crack interaction. Mechanisms such as stress-induced transformation and stress-induced microcracks, which involve the formation a process zone at the crack tip, are referred to as crack shielding. Mechanisms such as the residual microcracking and crack deflection are referred to as crack interaction. The residual microcracks occur as a consequence of anisotropic thermal expansion of non-cubic grains in single-phase materials or the differential thermal expansion between different phases in multi-phase materials. Crack interaction mechanisms do not involve the formation of a process zone.<sup>18,19</sup>

The objective of the present work was to measure the SENB toughness of a range of oxide ceramics with different microstructures and therefore different toughening mechanisms, by using various notch widths from 150 to 1800  $\mu\text{m}$ . A discussion is then given of the relationships between the SENB toughness and notch width, in conjunction with the operating mechanisms in the materials investigated.

## 2 Materials Investigated

Two types of oxide ceramics were selected for investigation, as shown in Table 1: (i) non-transformable alumina ceramics with three different grain sizes ( $\text{Al}_2\text{O}_3$ -I, II and III); (ii) transformation toughened ceramics with varying degrees of transformability, including  $\text{Y}_2\text{O}_3$ -stabilized tetragonal zirconia polycrystals (Y-TZP-I, II and III containing 2, 2.5 and 3 mol%  $\text{Y}_2\text{O}_3$ , respectively), MgO-partially stabilized zirconias (Mg-PSZ-I and II) and zirconia-toughened aluminas (Super-'Z' and ZTA). The alumina ceramics with various grain sizes were

fabricated by conventionally sintering a commercially available alumina powder (BACO 36RA, from BA Chemical Ltd, Bucks, UK) at temperatures of 1550 to 1650°C for various periods. The  $\text{Y}_2\text{O}_3$ -stabilized tetragonal zirconia polycrystals and Super-'Z' ceramics were made by sintering at 1550°C for 2 h the as-received  $\text{Y}_2\text{O}_3$ -stabilized zirconia powders (containing 2, 2.5 and 3 mol%  $\text{Y}_2\text{O}_3$ , respectively) and the mixed zirconia-alumina powder ( $\text{ZrO}_2$ -3 mol%  $\text{Y}_2\text{O}_3$  + 20 vol.%  $\text{Al}_2\text{O}_3$ ; Toyo Soda Manufacturing Co., Japan) respectively. MgO-partially stabilized zirconias were fabricated by sintering co-precipitated  $\text{ZrO}_2$ -9 mol% MgO at 1750°C for 2 h and thermally annealing at 1420°C for 5 h (Mg-PSZ-I) and 1100°C for 6 h (Mg-PSZ-II) respectively. The ZTA ceramic ( $\text{Al}_2\text{O}_3$ -15 vol.%  $\text{ZrO}_2$ ) was fabricated by sintering mixed alumina and zirconia powders which had been ball milled. The density of all the specimens was above 97% theoretical density. Typical microstructures of the sintered materials are summarized in Table 1 and Fig. 1.

The materials studied in this work were selected in order to vary the degree of stress-induced transformation toughening. Monolithic alumina ceramics do not exhibit any stress-induced phase transformation or the formation of a significant process zone because of their fine grain sizes ( $< 10 \mu\text{m}$ ).  $\text{Y}_2\text{O}_3$ -stabilized tetragonal zirconia polycrystals were considered to be the materials which exhibit the highest degree of stress-induced transformation. Transformability is controlled by such composition and microstructural parameters as  $\text{Y}_2\text{O}_3$  content and the grain size. Phase transformation of the retained tetragonal zirconia phase in the Super-'Z' and zirconia-toughened alumina (ZTA) ceramics differs from that in the Y-TZP ceramics, since  $\text{Al}_2\text{O}_3$  grains modify the shape of transformation zone.<sup>20</sup>

**Table 1.** Microstructural parameters of the materials investigated in this work

Materials	Composition	Average grain size ( $\mu\text{m}$ )	$\text{ZrO}_2$ Phases (%)	
			$\text{ZrO}_2$	As a whole
Alumina-I	$\text{Al}_2\text{O}_3$	2.6		
Alumina-II	$\text{Al}_2\text{O}_3$	4.2		
Alumina-III	$\text{Al}_2\text{O}_3$	6.3		
TZP-I (2Y)	$\text{ZrO}_2$ -2.0 mol% $\text{Y}_2\text{O}_3$	1.4	100 (t)	100 (t)
TZP-II (2.5Y)	$\text{ZrO}_2$ -2.5 mol% $\text{Y}_2\text{O}_3$	1.4	100 (t)	100 (t)
TZP-III (3Y)	$\text{ZrO}_2$ -3.0 mol% $\text{Y}_2\text{O}_3$	1.3	100 (t)	100 (t)
Mg-PSZ-I	$\text{ZrO}_2$ -9 mol% MgO	50		
Mg-PSZ-II	$\text{ZrO}_2$ -9 mol% MgO	50		
Super-'Z'	$\text{ZrO}_2$ -3.0 mol% $\text{Y}_2\text{O}_3$	1.0 ( $\text{ZrO}_2$ )		
	+ 20 vol.% $\text{Al}_2\text{O}_3$	1.2 ( $\text{Al}_2\text{O}_3$ )	100 (t)	80 (t)
ZTA	$\text{Al}_2\text{O}_3$ + 15 vol.% $\text{ZrO}_2$	1.6 ( $\text{ZrO}_2$ )	80 (t)	12 (t)
		2.8 ( $\text{Al}_2\text{O}_3$ )	20 (m)	3 (m)

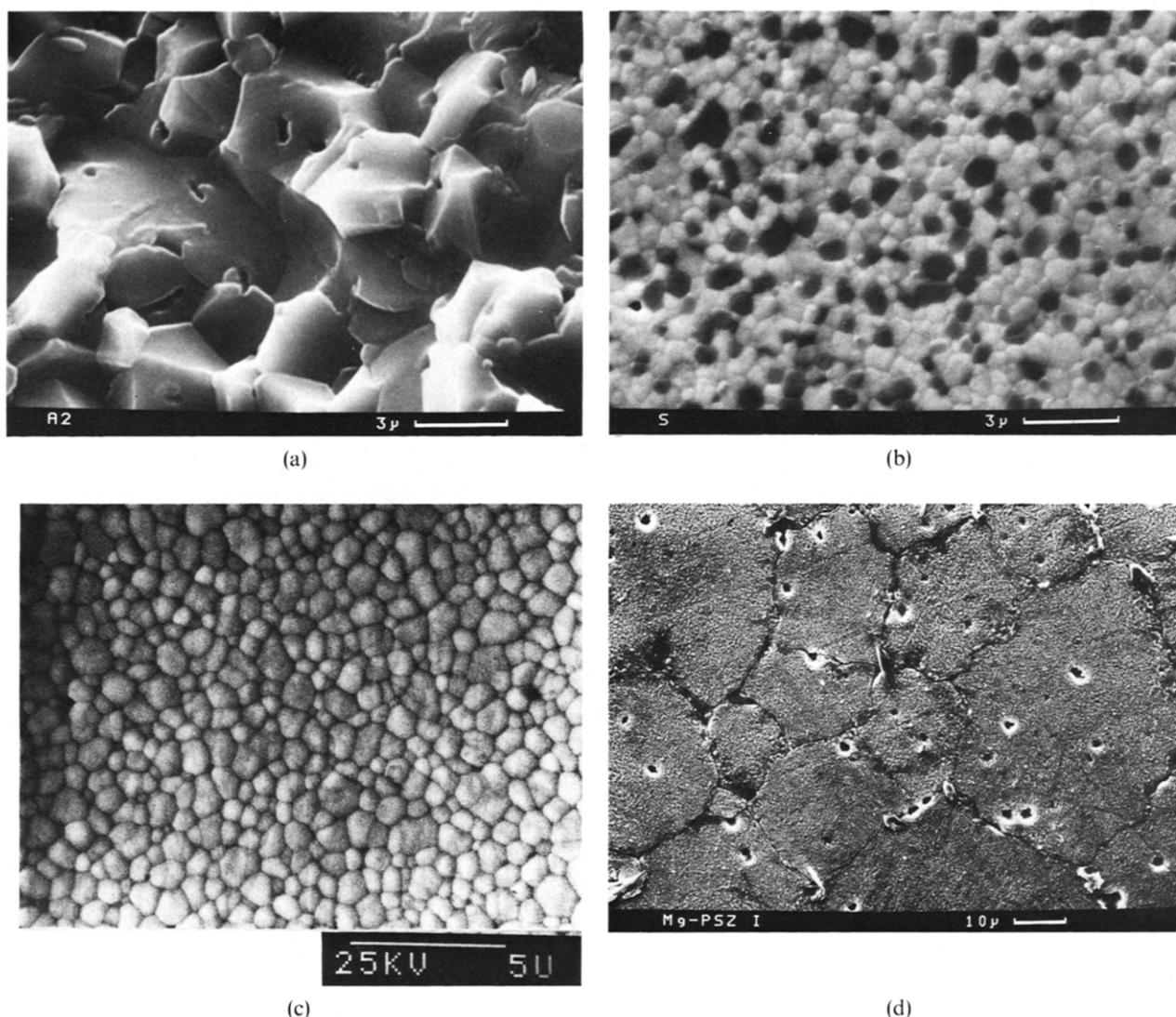


**Fig. 1.** SEM micrographs showing the microstructures of (a)  $\text{Al}_2\text{O}_3$ -II, (b) Super-'Z', (c) TZP-II containing 2.5 mol%  $\text{Y}_2\text{O}_3$  and (d) Mg-PSZ-I, ceramics, respectively. (a)  $\text{Al}_2\text{O}_3$  sintered at 1600°C for 4 h; (b) Super-'Z' sintered at 1550°C for 2 h; (c) TZP-II with 2.5 mol%  $\text{Y}_2\text{O}_3$  sintered at 1550°C for 2 h; (d) Mg-PSZ sintered at 1750°C for 2 h + 1420°C for 5 h.

The overall transformability (referred to as the volume fraction of transformable material in the process zone) of zirconia-toughened alumina ceramics is lower than that of Y-TZP and decreases with increasing  $\text{Al}_2\text{O}_3$  content. It is apparent that the ZTA exhibits less transformation toughening than the Super-'Z'. The transformation zone in the MgO-partially stabilized zirconias can be large as a consequence of their large grain size. In terms of the degree of transformation toughening, the materials selected in the present work may be listed as:

$$\text{Y-TZP} > \text{Mg-PSZ} > \text{Super-'Z'} > \text{ZTA} > \text{Aluminas} \quad (1)$$

SENB toughness measurements were carried out on specimens in the form of three-point bend bars with dimensions of  $4.0 \times 5.0 \times 20$  mm at a crosshead speed of 0.5 mm/min. Notches of various widths

were introduced by using diamond blades (saws). The calibration factor proposed by Brown & Srawley<sup>21</sup> was used to calculate the SENB toughness on the basis of experimental results. The as-notched samples were not thermally treated, in order that any machining effects at the notch tip might be studied.

### 3 The Transformation Zone at Notch Tip

A transformation zone will be introduced at each notch tip as a result of the mechanical stress from the diamond blade, the shape and dimensions of which will be determined by the geometry and size of the diamond blade employed. It was observed that all the notches exhibited a near semicircular tip. On the basis of this assumption, Fig. 2, it can be geometri-

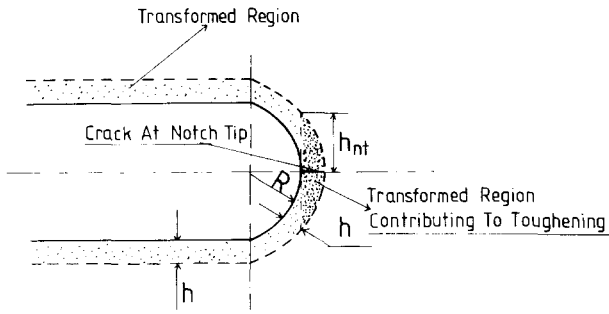


**Fig. 2.** A diagrammatic representation of the transformation zone at notch tip, where  $R$  is the radius of the notch tip,  $h$  the transformation thickness induced by diamond blade, and  $h_{nt}$  is the effective transformation zone width at the notch tip.

cally shown that the transformation zone width  $h_{nt}$  at the notch tip increases with increasing notch width  $R$ , and may be expressed as:

$$h_{nt} = (2hR + h^2)^{0.5} \quad (2)$$

Where  $h$  is the thickness of the transformed region (determined by the transformability of the material and the roughness and machining speed of the diamond blade), caused by the diamond blade at notch tip.

The two limiting cases are:

$$h_{nt} = (2hR)^{0.5} \quad (3)$$

when  $R \gg h$ , which is the case when conventional diamond blades are used to introduce notches; and

$$h_{nt} = h \quad (4)$$

when  $R \rightarrow 0$ , which is similar to the situation when the samples are pre-cracked, e.g. by fatigue.

It has been demonstrated that the fracture toughness of transformation toughened ceramics is related to the size of the transformation zone and the volume fraction of stress-induced transformable tetragonal zirconia phase in the process zone.<sup>14-16</sup> According to McMeeking, Evans and Swain,<sup>14,16</sup> the fracture toughness due to stress-induced transformation may be written as:

$$K = \eta E \Delta V V_f (h_t)^{0.5} / (1 - \nu) \quad (5)$$

and therefore:

$$K = \eta E \Delta V V_f (2hR + h^2)^{0.25} / (1 - \nu) \quad (6)$$

where  $E$  and  $\nu$  are the elastic modulus and Poisson's ratio of the material,  $\Delta V$  the volume expansion associated with the transformation,  $V_f$  the volume fraction of stress-induced transformable tetragonal phase in the process zone,  $h_t$  the width of the transformation zone and  $\eta$  is a constant determined by the nature of the transformation.

Combining eqns (6) and (3) for the case when

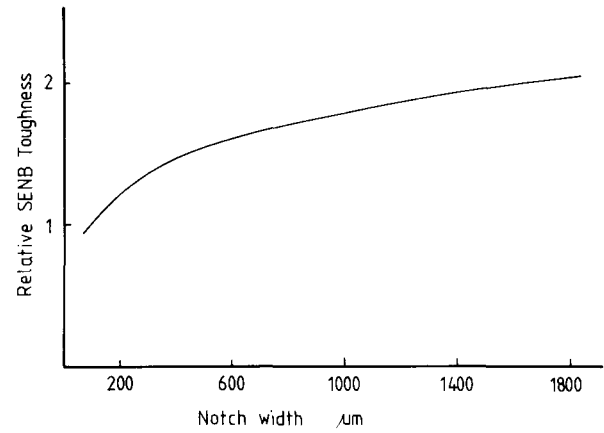


**Fig. 3.** The theoretically expected dependence of SENB toughness on notch width for transformation toughened ceramics when  $R \gg h$ , which is applicable to the notch widths introduced by conventional diamond blades.

$R \gg h$ , which is applicable to the experimental parameters selected in the present work,

$$K = \eta E \Delta V V_f (2hR)^{0.25} / (1 - \nu) \quad (7)$$

The above equations imply that the SENB toughness increases with increasing notch width ( $R$ ) and increasing transformability of materials to be tested (represented by  $V_f$  and  $h$ ). As the minimum notch width introduced by conventional diamond machining techniques is likely to be  $> 100 \mu\text{m}$ , which is much larger than the transformation zone width (5 to  $10 \mu\text{m}$ ) in  $\text{Y}_2\text{O}_3$ -stabilized tetragonal zirconia polycrystals and zirconia-toughened alumina ceramics,<sup>20</sup> the measured SENB toughness will be proportional to  $R^{0.25}$ . Consequently, it can be predicted that the SENB toughness of transformation toughened ceramics may double in value when the notch width is increased from 150 to  $1600 \mu\text{m}$  (Fig. 3).

## 4 Results and Discussions

### 4.1 Alumina ceramics

Figures 4, 5 and 6 show the SENB fracture toughness as a function of notch width for the three alumina ceramics with different grain sizes. It may be seen that SENB toughness decreases slightly with increasing notch width from 200 to  $1800 \mu\text{m}$ . It is also apparent that the SENB toughness increases slightly with increasing grain size, from 2.6 to more than  $6.0 \mu\text{m}$ . This trend agrees well with the results obtained by Rice *et al.*<sup>22,23</sup> The increase in fracture toughness with grain size in alumina ceramics has been suggested to be due to the residual strain energy developed as a result of the anisotropy in thermal expansion of the hexagonal alumina grains.

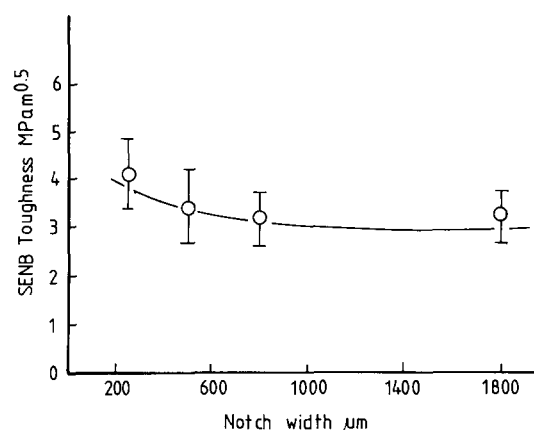


Fig. 4. The SENB toughness as a function of notch width for alumina-I, indicating a slight decrease in the SENB toughness with increasing notch width.

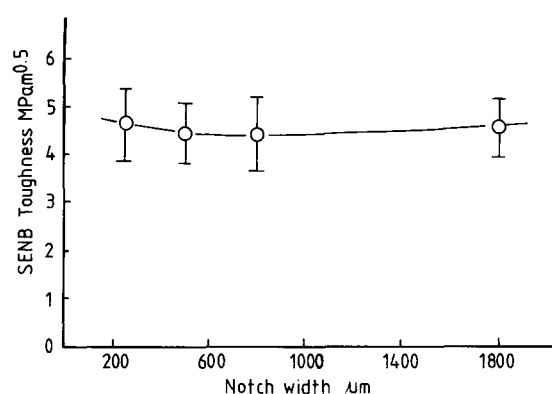


Fig. 5. The SENB toughness as a function of notch width for alumina-II.

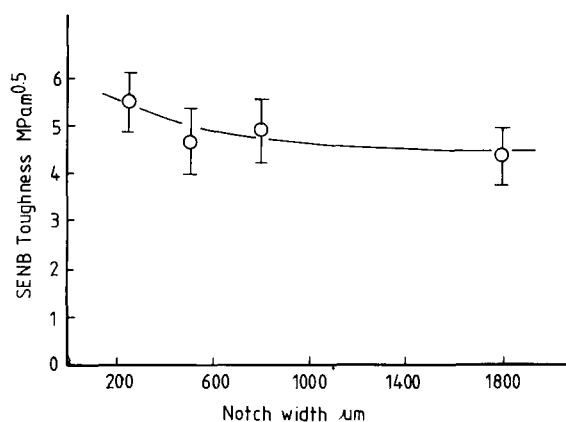


Fig. 6. The SENB toughness as a function of notch width for alumina-III.

The residual strain energy may promote microcracking and *R*-curve behaviour.<sup>23</sup>

The fracture toughness of alumina ceramics is closely related to such microstructural parameters as grain size, grain morphology and grain boundary characteristics, where grain size is the dominant factor.<sup>24</sup> The grain size dependence of fracture toughness for a constant notch width in alumina ceramics has been well established both theoretically

and experimentally.<sup>22,23</sup> The fracture toughness is almost independent of grain size at the small grain size range ( $< 15 \mu\text{m}$ ) and shows a steady increase in the intermediate grain size range (30 to  $50 \mu\text{m}$ ), as a result of the presence of residual strain energy. A maximum in fracture toughness is then observed in the intermediate grain size range, where the maximum amount of residual strain energy may be retained without causing spontaneous microcracking. This is followed by a fall in toughness with further increase in grain size. Theoretically, anisotropic thermal expansion is typical of all non-cubic materials, including alumina, hafnia, and mullite ceramics.<sup>24</sup> The grain size dependence of the fracture toughness is attributed to the strain energy associated with the stresses generated by the anisotropic thermal expansion of the non-cubic grains on cooling from the sintering temperature. The residual strain energy stored in each grain due to the anisotropic thermal expansion increases with increasing grain facet length and therefore with grain size, although the residual stresses are independent of grain size.<sup>25-27</sup> The maximum differential grain boundary strain was shown to be simply proportional to the product of the maximum difference in thermal expansion coefficient (between *a*- and *c*-axes) and the temperature difference ( $\Delta T$ ) between ambient and the temperature below which plastic deformations become negligible ( $1000^\circ\text{C}$  for most ceramic materials).<sup>24</sup>

Three distinct microstructures can therefore be obtained in relation to the grain size:

- (i) fine grain sized alumina ceramics ( $< 15 \mu\text{m}$ ), which contain a limited amount of residual strain energy;
- (ii) intermediate grain sized alumina ceramics (30– $50 \mu\text{m}$ ), in which there exists a considerable amount of residual strain energy, but which is insufficient to cause spontaneous microcracks on cooling from the sintering temperature;
- (iii) large grain sized alumina ceramics ( $> 70 \mu\text{m}$ ), in which the residual strain energy is sufficient to cause spontaneous cracking on cooling from the fabrication temperature.

It is generally observed that the fine grain sized alumina ceramics exhibit intergranular fracture, and that the intermediate and coarse grain sized alumina ceramics exhibit intragranular fracture. For complete fracture of a single grain boundary facet, two conditions must be satisfied:<sup>24,27</sup> (a) the elastic strain energy around the facet must equal or be greater than the energy required to fracture the grain

boundary; and (b) a flaw of sufficient size is also needed in order to give a high enough stress concentration for fracture to proceed.

The SENB toughness of the intermediate grain sized alumina ceramics is of interest, since a stress-induced microcrack zone is developed when an externally applied stress is superimposed on the existing residual stresses.<sup>22,23</sup> It is expected that this type of material exhibits considerable SENB toughness dependence on the notch width. Strong *R*-curve behaviour has been reported for this type of alumina ceramic.<sup>17,18</sup> It has been suggested that grain bridging or internal friction is also partially responsible for the increase in toughness with increasing crack length.<sup>12</sup> Stress-induced microcracks in the intermediate grain sized alumina ceramics and the residual microcracks in the large grain sized alumina ceramics differ fundamentally in their response to SENB testing. The residual microcracks contribute to fracture toughness via crack branching or deflection, which are crack interaction processes. On the other hand, the fine grained alumina ceramics may not be so fundamentally different from the intermediate grained alumina ceramics in terms of stress-induced microcrack zone. It has been reported that a measurable microcrack zone occurs at the notch tip in materials with grain sizes as small as 2  $\mu\text{m}$ .<sup>22,28,29</sup> This may contribute to the rising SENB toughness with increasing notch width for the fine grained materials.<sup>30,31</sup> There exists a sharp rise in the density of stress-induced microcracks at the notch tip in the grain size range 15 to 30  $\mu\text{m}$ .<sup>22,28</sup> The alumina ceramics investigated in this work are considered to be fine grain sized materials, in which the internal residual strains may not be large enough to cause an extended microcrack zone even when an externally applied stress is superimposed on the notch tip, although a limited microcrack zone may be induced at the notch tip.

In theory, SENB toughness of all the brittle materials increases with rising notch width, independent of toughening mechanisms involved at the notch tip.<sup>32,33</sup> This is a consequence of the reduced stress intensity when large notches are introduced. However, notch width is not the only factor affecting the SENB toughness value measured for a given ceramic material. In practice, it is impossible to guarantee that all the notches are exactly the same shape. The damage caused by the diamond blade at the notch tip may vary from one specimen to another. It is likely that the slight decrease in SENB toughness with increasing notch width shown in Figs 4, 5 and 6 is a result of the non-uniform notch tip and the varying degree of machining damage

induced at the notch tip. An increased degree of machining damage is expected in those samples containing the large notches, because the blades used in the machining operation contained a coarse abrasive. The difference both in the degree of machining damage to the notch tip and in the notch tip profile introduced may also be helpful in explaining the contradicting results for the similar materials investigated by some previous researchers. For example, both Bertolotti<sup>30</sup> and Pabst<sup>31</sup> observed increasing SENB toughness with rising notch width for sintered alumina ceramics with average grain sizes of 10  $\mu\text{m}$ . Mussler *et al.*<sup>28</sup> noted increasing SENB toughness with rising notch width for 2–5  $\mu\text{m}$  grain sized aluminas.

#### 4.2 TZP ceramics

In Figs 7, 8 and 9 the SENB toughness is plotted as a function of notch width for the three  $\text{Y}_2\text{O}_3$ -

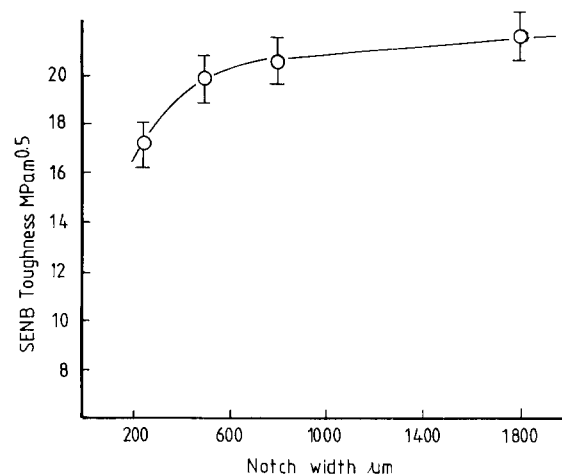


Fig. 7. The SENB toughness dependence of notch width for TZP-I containing 2 mol%  $\text{Y}_2\text{O}_3$ . The SENB toughness increases dramatically when the notch width is increased from 200 to 700  $\mu\text{m}$ . Further increase in the notch width has little effect on the toughness.

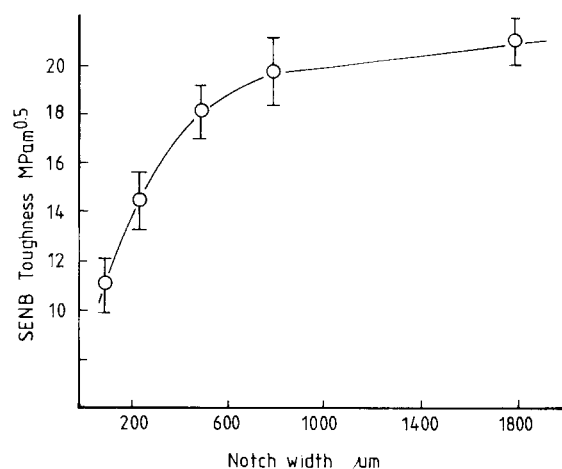
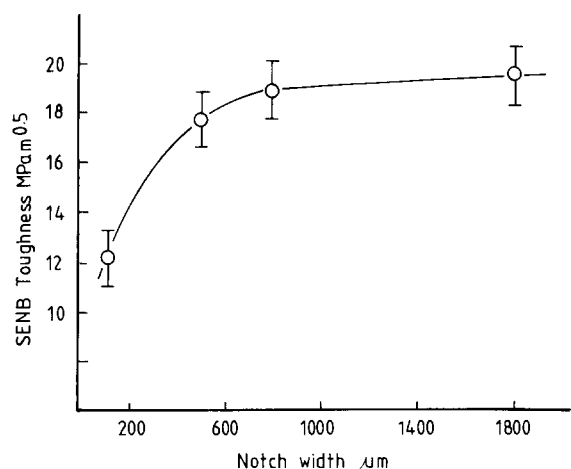


Fig. 8. The SENB toughness as a function of notch width for TZP-II containing 2.5 mol%  $\text{Y}_2\text{O}_3$ .



**Fig. 9.** The SENB toughness as a function of notch width for TZP-III containing 3 mol%  $Y_2O_3$ . The SENB toughness almost doubles its value when notch width is increased from 150 to 1800  $\mu m$ . This is consistent with the theoretically expected result in Fig. 3.

stabilized tetragonal zirconia polycrystals containing 2.0, 2.5 and 3.0 mol%  $Y_2O_3$ , respectively. It is apparent that they all show a similar trend in terms of the relationship between SENB toughness and notch width, although they exhibit different transformabilities. There is a dramatic increase in the SENB toughness when the notch width is increased from 150 to 700  $\mu m$ . Further increases in notch width result in little change. The SENB toughness of Y-TZP containing 2.5 and 3 mol%  $Y_2O_3$  almost doubles in value when the notch width is increased from 150 to 1600  $\mu m$ . This is consistent with the predicted result shown in Fig. 3. At small notch widths, the TZP containing 2 mol%  $Y_2O_3$  shows a higher SENB toughness than the TZP containing 2.5 and 3 mol%  $Y_2O_3$ . However, the overall increase in the SENB toughness for this material with increasing notch width is smaller than for the TZP containing 2.5 and 3 mol%  $Y_2O_3$ . The increased degree of machining damage at the notch tip by the thick diamond blades to this highly transformable material (TZP-2Y is more readily transformable than TZP-2.5Y and TZP-3Y) can account for this behaviour. Microcracks may also be present at the notch tip when large notch widths are introduced to the TZP containing 2 mol%  $Y_2O_3$ . For a given notch width, the SENB toughness follows the order of TZP-2Y > TZP-2.5Y > TZP-3Y. This is consistent with the indentation toughness results for these materials having equivalent grain size.<sup>3</sup>

### 4.3 Mg-PSZ ceramics

Figures 10 and 11 show the SENB toughness as a function of notch width for the two MgO-partially stabilized zirconias (Mg-PSZ-I and II). Again, the

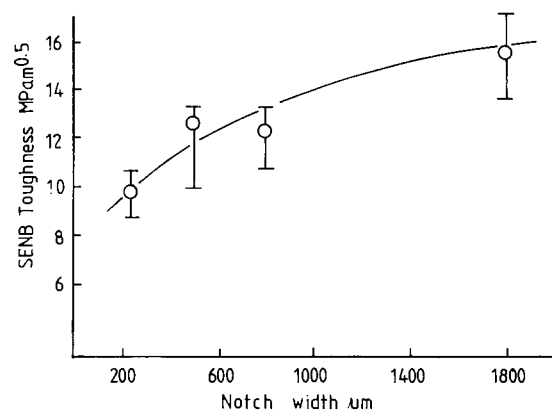


**Fig. 10.** The SENB toughness as a function of notch width for Mg-PSZ-I, showing a steady increase in the SENB toughness with increasing notch width from 200 to 1800  $\mu m$ .

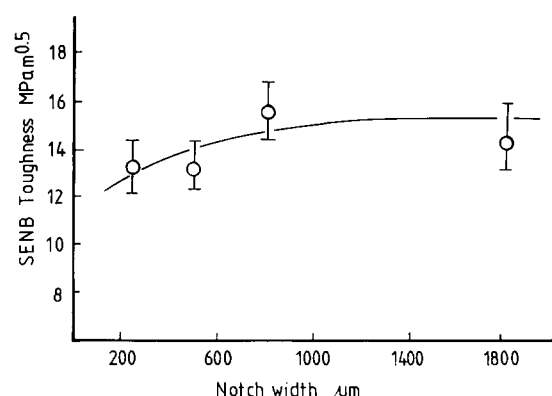


**Fig. 11.** The SENB toughness as a function of notch width for Mg-PSZ-II.

SENB toughness increases steadily with increasing notch width in the region of 150 to 1800  $\mu m$ . In contrast to the Y-TZP ceramics in Figs 7, 8 and 9, the Mg-PSZ exhibit a further increase in SENB toughness when the notch width is increased from 1000 to 1800  $\mu m$ .

### 4.4 ZTA ceramics

In Figs 12 and 13, the SENB toughness is shown as a function of notch width for the Super-'Z' and ZTA ceramics, respectively. As with the Y-TZP and the Mg-PSZ ceramics already discussed, their SENB toughness increases with increasing notch width from 150 to 1800  $\mu m$ . However, the overall increase is much smaller than for those of the Y-TZP and Mg-PSZ ceramics.

### 4.5 General discussions

Equations (5) and (7) imply that an increase in notch width will result in an increase in SENB toughness for transformation toughened ceramics. When comparing Fig. 3 and Figs 7 to 13, it is readily recognized that the experimental results for all the transformation toughened ceramics investigated in



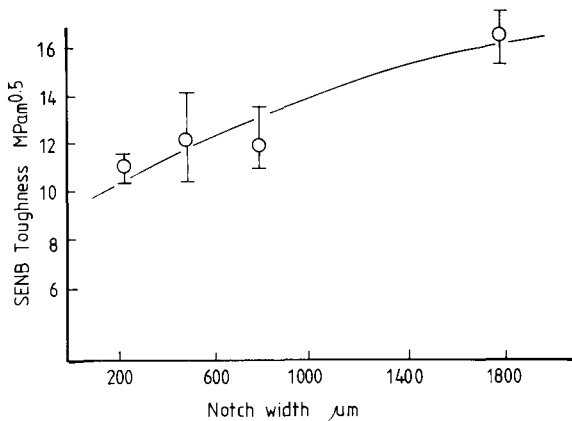


**Fig. 12.** The SENB toughness is plotted as a function of notch width for the Super-'Z' ceramic. The overall increase in the SENB toughness is smaller than that in Y-TZP ceramics shown in Figs 5, 6 and 7, as a consequence of the reduced volume fraction of transformable tetragonal phase in the process zone.

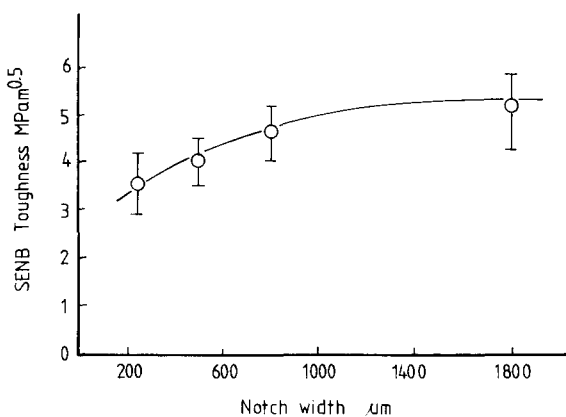


**Fig. 13.** The SENB toughness is shown as a function of notch width for the zirconia-toughened alumina (ZTA), indicating a much smaller overall increase in the SENB toughness than for Y-TZP.

the present work follow the theoretically predicted trend, although it is difficult to compare the absolute data. It can therefore be postulated that the apparent increase in SENB toughness with increasing notch width for Y-TZP, Mg-PSZ, and ZTA ceramics shown in Figs 7 to 13 is due to the extended transformation zone at the notch tip. On the other hand, the difference in transformability among these materials leads to a different response to varying notch width from one material to another. The overall increase in SENB toughness with increasing notch width follows the sequence in eqn (1). This is consistent with the difference in microstructure and transformability between these materials. As is indicated by the amount of tetragonal phase present in each material shown in Table 1, the Y-TZP ceramics exhibit the highest transformability among the materials investigated in the present work. The second most transformable materials are the Mg-PSZ. The substitution of tetragonal  $\text{ZrO}_2$  phase by

$\text{Al}_2\text{O}_3$  in the zirconia-toughened ceramics (Super-'Z' and ZTA) will apparently reduce the percentage of tetragonal phase present in whole structure. Their transformability is therefore decreased. This is shown both by the reduced fracture toughness and the enhanced thermal stability when compared with the Y-TZP ceramics.<sup>1,3</sup> It is likely that both the volume fraction of stress-induced transformable metastable tetragonal zirconia phase in the process zone ( $V_f$ ) and the transformation zone thickness at the notch tip ( $h$ ) will be reduced in these dispersion-toughened ceramics, possibly as a result of the suppression in the autocatalytic nature of the martensitic  $\text{ZrO}_2(\text{t})$  to  $\text{ZrO}_2(\text{m})$  transformation by the presence of non-transformable inclusions.<sup>34,35</sup> For the monolithic alumina ceramics, as shown in Figs 4, 5 and 6, an increase in notch width does not cause an increase in the SENB toughness. Instead, the increased degree of the machining damage at notch tip in the samples containing large notches results in a slight decrease in SENB toughness in these non-transformable materials.

The analytical and experimental results outlined clearly demonstrate the effects of transformation zone width on the SENB toughness in Y-TZP, Mg-PSZ and ZTA ceramics. An over-estimated SENB value is obtained in these toughened ceramics if an extended transformation zone width is mechanically introduced at the notch tip. To a certain extent, the over-estimated SENB values may not truly represent the fracture toughness of these materials, as such large transformation zones ( $> 600 \mu\text{m}$ ) may never be achieved at the tip of sharp cracks. In Y-TZP and ZTA ceramics, the transformation zone width is often limited to  $< 10 \mu\text{m}$  at the crack tip, as shown by Wang *et al.*<sup>36</sup> by property measurement and by Ruhle *et al.*<sup>20</sup> using HRTEM observation. In  $\text{CeO}_2$ -stabilized tetragonal zirconia polycrystals (Ce-TZP), however, large transformation zones do occur at the crack tip. Investigations recently carried out on Ce-TZP have shown that both the shape and size of transformation zones in these materials differ considerably from those in Y-TZP. The transformation zone in the former is much elongated and could be more than ten times larger than that in the latter.<sup>35,37,38</sup> This may make Ce-TZP fundamentally different from other transformation toughened ceramics and explains why Ce-TZP exhibit a much higher fracture toughness than Y-TZP.<sup>34,35</sup> In a simple sense, it can also be appreciated that a fracture toughness value comparable to that of Ce-TZP can be achieved in Y-TZP, if the transformation zone induced at the notch tip has a dimension similar to that at the crack tip in Ce-TZP. The

effective transformation zone in Y-TZP ceramics can be extended up to  $600\text{ }\mu\text{m}$ , i.e. a transformable grain could contribute to the final toughening even when at a distance of  $600\text{ }\mu\text{m}$  away from the tip of the propagating crack.

On the basis of these discussions it is of interest to consider the 'stress-free SENB toughness' for transformation toughened ceramics. As discussed earlier, the size of transformation zone at the notch tip increases with increasing notch width. The level of residual stress associated with the transformation at the notch tip increases accordingly. Figures 7 to 13 show the rising SENB toughness with increasing notch width, as a consequence of the increasing transformation zone width or residual stress level. It is therefore meaningful to work out the 'stress-free SENB toughness' by extrapolating the notch width to zero in Figs 7 to 13. The resultant SENB toughness is 12, 8.5, 8, 7.5, 11, 9 and  $2.7\text{ MPam}^{0.5}$  for Figs 7 to 13, respectively. These values are close to those measured on the specimens which were thermally treated at  $1250^\circ\text{C}$  for 1 h to remove the residual transformation zone at the notch tip after a  $200\text{ }\mu\text{m}$  notch was introduced.

Figure 14 shows the SENB toughness as a function of notch length/width ratio,  $c/d$ , for the Y-TZP ceramic containing 2 mol%  $\text{Y}_2\text{O}_3$ . It is clear that the SENB toughness is almost independent of notch length even for this highly transformation toughened ceramic. As was shown in Fig. 2, there exists a transformation thickness ( $h$ ) on both of the notched surfaces along the notch length. However, the transformation in these regions does not contribute to the toughening occurring at the notch tip, as any volume expansion and shear strain will be offset by the free space associated with the notch. In this respect, the mechanically notched samples are completely different from the pre-cracked samples,

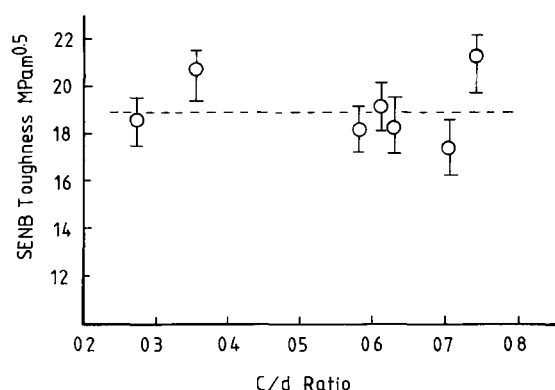


**Fig. 14.** The SENB toughness dependence on the notch length/width ratio,  $c/d$ , for TZP-2 mol%  $\text{Y}_2\text{O}_3$  ceramic, illustrating that the SENB toughness is almost independent of the notch length even for the highly transformation toughened ceramic.

where the fracture toughness increases with increasing crack length, known as *R*-curve behaviour.<sup>1</sup>

## 5 Conclusions

Fine grain sized alumina ceramics show little change in SENB toughness with increasing notch width. The slight decrease is probably due to the degree of machining damage when the notched samples were prepared. In contrast, all the transformation toughened ceramics, including Y-TZP, Mg-PSZ and ZTA ceramics, show a strong SENB toughness dependence on notch width. This agrees well with the theoretical analysis which considers the over-estimate in SENB toughness due to the enlarged transformation zone developed with increasing notch width. However, the overall increase in SENB toughness for ZTA ceramics is smaller than for Y-TZP and is below the value predicted theoretically, as a consequence of the reduced transformability in these materials. On the other hand, the SENB toughness is not sensitive to the notch length even for highly transformation toughened ceramics. The experimental results in this work also implying that the fracture toughness of Y-TZP ceramics would be comparable to that of Ce-TZP ceramics, if their transformation zone could be effectively extended.

## Acknowledgement

The authors wish to thank Dr Roger Morrell of the National Physical Laboratory, Teddington, for his involvement in preparing some of the notched specimens.

## References

1. Evans, A. G. & Cannon, R. M., Toughening of brittle solids by martensitic transformations. *Acta Metall.*, **34** (1986) 761–800.
2. Lange, F. F., Transformation toughening., *J. Mat. Sci.*, **17** (1982) 225–46.
3. Claussen, N., Microstructural design of zirconia-toughened ceramics (ZTC). In *Advances in Ceramics*, Vol. 12, *Science and Technology of Zirconia II*, ed. N. Claussen, M. Ruhle & A. H. Heuer. The American Ceramics Society, Columbus, OH, 1984, pp. 325–51.
4. Larsen, D. C., Adams, J. W., Johnson, L. R., Teotia, A. P. & Hill, L. G., Ceramic materials for advanced heat engines. Noyes Publications, NJ, 1985.
5. Butler, E. G., Engineering ceramics: applications and testing requirements. In *Mechanical Testing of Engineering Ceramics at High Temperatures*, ed. B. F. Dyson, R. D.

- Mohr & R. Morrell. Elsevier Applied Science, London, 1989, pp. 1–10.
6. Munz, D., Effect of specimen type on the measured fracture toughness of brittle ceramics. In *Fracture Mechanics of Ceramics*, Vol. 6, ed. R. C. Bradt, A. G. Evans, D. H. P. Hasselman & F. F. Lange, Plenum Press, NY, 1983, pp. 1–26.
  7. Loveday, M. S. & Morrell, R., Standardisation of mechanical testing and quality control. In *Mechanical Testing of Engineering Ceramics at High Temperatures*, ed. B. F. Dyson, R. D. Mohr & R. Morrell. Elsevier Applied Science, London, 1989, pp. 11–30.
  8. Anstis, G. R., Chantikul, P., Lawn, B. R. & Marshall, D. B., A critical evaluation of indentation techniques for measuring fracture toughness, I: Direct crack measurement. *J. Amer. Ceram. Soc.*, **64** (1981) 533–8.
  9. Paterson, A. W. & Stevens, R., Comparison of indentation and notched bar toughness of TZP ceramics: Relevance to models of the fracture process. *Intl J. High. Tech. Ceram.*, **2** (1986) 211–29.
  10. Pabst, R. F., Steeb, J. & Claussen, N., Microcracking in a process zone and its relation to continuum mechanics. In *Fracture Mechanics of Ceramics*, Vol. 4, ed. R. C. Bradt, D. H. P. Hasselman & F. F. Lange. Plenum Press, NY, 1978, pp. 821–34.
  11. Chen, I. W., Implication of transformation plasticity on deformation and fracture control of zirconia containing ceramics. In *Zirconia Ceramics 7*, ed. S. Somiya & M. Yoshimura. Uchida Rokakuho, Tokyo, Japan, 1985, pp. 49–63.
  12. Wieninger, H., Kromp, K. & Pabst, R. F., Crack resistance curves of alumina and zirconia at room temperature. *J. Mat. Sci.*, **26** (1986) 411–18.
  13. Rief, C. & Kromp, K., Fracture toughness testing. In *Mechanical Testing of Engineering Ceramics at High Temperatures*, ed. B. F. Dyson, R. D. Mohr & R. Morrell. Elsevier Applied Science, London, 1989, pp. 209–26.
  14. McMeeking, R. & Evans, A. G., Mechanisms of transformation toughening in brittle materials. *J. Amer. Ceram. Soc.*, **65** (1982) 242–6.
  15. Evans, A. G., Toughness/microstructure interactions. In *Fracture in Ceramic Materials*, ed. A. G. Evans. Noyes Publications, NJ, 1984, pp. 1–5.
  16. Swain, M. V., Inelastic deformation of Mg-PSZ and its significance for strength–toughness relationships in zirconia toughened ceramics. *Acta Metall.*, **33** (1985) 2083–91.
  17. Evans, A. G., Toughening mechanisms in zirconia alloys. In *Advances in Ceramics*, Vol. 12, *Science and Technology of Zirconia II*, ed. N. Claussen, M. Ruhle & A. H. Heuer. The American Ceramics Society, Columbus, OH, 1984, pp. 193–212.
  18. Evans, A. G., Toughening mechanisms in zirconia alloys. In *Fracture in Ceramic Materials*, ed. A. G. Evans. Noyes Publications, NJ, 1984, pp. 16–55.
  19. Evans, A. G. & Fu, Y., The mechanical behaviour of alumina: a model anisotropic brittle solid. In *Fracture in Ceramic Materials*, ed. A. G. Evans. Noyes Publications, NJ, 1984, pp. 56–88.
  20. Ruhle, M., Kraus, B., Strecker, A. & Waidelich, D., In-situ observation of stress-induced phase transformations in zirconia containing ceramics. In *Advances in Ceramics*, Vol. 12, *Science and Technology of Zirconia II*, ed. N. Claussen, M. Ruhle & A. H. Heuer. The American Ceramics Society, Columbus, OH, 1984, pp. 256–74.
  21. Brown, W. F. & Srawley, J. E., Plane strain crack toughness testing of high strength metallic materials. ASTM Special Technical Publications, Vol. 410, 1966.
  22. Rice, R. W., Freiman, S. W. & Becher, P. F., Grain size dependence of fracture energy in ceramics, I: Experiment. *J. Amer. Ceram. Soc.*, **64** (1981) 345–50.
  23. Rice, R. W. & Freiman, S. W., Grain size dependence of fracture energy in ceramics, II: A model for non-cubic materials. *J. Amer. Ceram. Soc.*, **64** (1981) 350–4.
  24. Davidge, R. W., Cracking at grain boundaries in polycrystalline brittle materials. *Acta Metall.*, **29** (1981) 1695–702.
  25. Evans, A. G. & Charles, E. A., Fracture toughness determination by indentation. *J. Amer. Ceram. Soc.*, **59** (1976) 371–2.
  26. Evans, A. G. & Fu, Y., Spontaneous microcracking in microstructural residual stress. In *Fracture in Ceramic Materials*, ed. A. G. Evans. Noyes Publications, NJ, 1984, pp. 154–70.
  27. Evans, A. G. & Fu, Y., Induced microcracking: Effect of applied stress. In *Fracture in Ceramic Materials*, ed. A. G. Evans. Noyes Publications, NJ, 1984, pp. 171–89.
  28. Mussler, B., Swain, M. V. & Claussen, N., Dependence of fracture toughness of alumina on grain size and test technique. *J. Amer. Ceram. Soc.*, **65** (1982) 566–72.
  29. Claussen, N., Mussler, B. & Swain, M. V., Grain size dependence of fracture energy in alumina. *J. Amer. Ceram. Soc.*, **65** (1982) C-14–16.
  30. Bertolotti, R. L., Fracture toughness of polycrystalline alumina. *J. Amer. Ceram. Soc.*, **56** (1973) 107.
  31. Pabst, R. F., Determination of  $K_{Ic}$ -factors with diamond saw cuts in ceramic materials. In *Fracture Mechanics of Ceramics*, Vol. 2, ed. R. C. Bradt, D. H. P. Hasselman & F. F. Lange. Plenum Press, NY, 1974, pp. 555–66.
  32. Weiss, V., Notch analysis of fracture. In *Fracture III*, ed. H. Liebowitz. Academic Press, NY, 1971, pp. 227–64.
  33. Rice, J. R., Mathematical analysis in the mechanics of fracture. In *Fracture II*, ed. H. Liebowitz. Academic Press, NY, 1968, pp. 191–311.
  34. Reyes-Morel, P. E. & Chen, I. W., Transformation plasticity of CeO<sub>2</sub> stabilized tetragonal zirconia polycrystals, I: Stress assistance and autocatalysis. *J. Amer. Ceram. Soc.*, **71** (1988) 343–53.
  35. Reyes-Morel, P. E., Cherng, J. & Chen, I. W., Transformation plasticity of CeO<sub>2</sub> stabilized tetragonal polycrystals, II: Pseudoelasticity and shape memory effect. *J. Amer. Ceram. Soc.*, **71** (1988) 648–57.
  36. Wang, J., Rainforth, M. & Stevens, R., The grain size dependence of mechanical properties in Y-TZP ceramics. *J. Trans. Brit. Ceram. Soc.*, **88** (1988) 1–5.
  37. Yu, C. S. & Shetty, D. K., Transformation yielding, plasticity, and crack growth resistance (*R*-curve) behaviour of CeO<sub>2</sub>-TZP. *J. Mat. Sci.*, **25** (1990) 2025–35.
  38. Yu, C. S. & Shetty, D. K., Transformation zone shape, size, and crack growth resistance (*R*-curve) behaviour of ceria partially stabilized zirconia polycrystals. *J. Amer. Ceram. Soc.*, **72** (1989) 921–8.